Original Article

A histological and immunohistochemical study of the effect of platelet-rich plasma on a corneal alkali burn in adult male albino rat

Heba E. M. Sharaf Eldin, Marwa A. A. Ibrahim and Noha R. M. Elswaidy

Department of Histology and Cell Biology, Faculty of Medicine, Tanta University

ABSTRACT

Background: Ocular chemical injuries are an emergency that needs immediate and intensive evaluation and treatment. Platelet- rich plasma (PRP) has become a common treatment in the field of ophthalmological surgery.

Aim of the study: to evaluate and compare the alleviating effect of a single dose of PRP injection applied either after 2 hours or 48 hours on an alkali-induced corneal burn.

Materials and Methods: Thirty adult male albino rats were equally divided into 5 groups; Control, PRP group, alkali-burn group, alkali-burn+ PRP-treated after 2hours group and alkali-burn+ PRP-treated after 48hours group. Corneal specimens were processed for different histological and immunohistochemical techniques.

Results: Alkali burnt cornea revealed focal discontinuity and denudation of corneal epithelium alternating with focal disorganization and stratification. Bowman's membrane appeared irregular with focal disruption. The Descemet's membrane appeared thinned out and disrupted. Mononuclear cellular infiltration and invasion with small blood vessels were observed. Upon intervention with PRP after 2hours of alkali-burn, a near normal corneal histological structure was observed. Yet upon intervention with PRP after 48hours of alkali-burn, a disturbed corneal histological structure with vacuolated epithelium and some nuclear changes were detected. A highly significant difference in the immunohistochemical staining for detection of P53, Ki67, MMP-1 and MMP-9 was detected upon alkali burn compared to the control, whereas a non-significant difference was observed in group IV compared to the control group, yet a significant difference was detected between group V and the control group.

Conclusion: A single dose PRP injection had an effective alleviating effect on alkali-induced corneal burn, yet the PRP injection after 2hours of the burn was more efficient in restoring the corneal healthy surface rather than its application after 48 hours.

Received: 03 January 2019, **Accepted:** 10 Feburary 2019

Key Words: Alkali-burn; cornea; immunohistochemistry; PRP.

Corresponding Author: Marwa A. A. Ibrahim, MD, Histology Department, Faculty of Medicine, Tanta University, 31527 Tanta, Egypt, 44519, Egypt, **Tel.**: +20 10 9918 6399, **E-mail:** maleox68@yahoo.com, marwa.ibrahim@med.tanta.edu.eg

ISSN: 1110-0559, Vol. 42, No. 2

INTRODUCTION

Ocular chemical injuries are an emergency that needs immediate and intensive evaluation and treatment. These injuries are common among chemical laboratories and construction workers. The damage resulting from chemical injuries could be so severe leading to opacification, neovascularization of the cornea and acute increase in intraocular pressure due to shrinkage and contraction of the cornea[1].

The corneal ulcer resulting from an alkali-burn is an epithelial defect, with loss of stroma, stromal inflammation or a combination. Alkali substances are lipophilic agents that penetrate the eye more rapidly, thus they are even more harmful than acids[1,2].

After chemical injury, the aim of therapy is to restore a normal ocular surface and corneal clarity. Limbal grafts are the common choice in treatment of this severe disorder. However, their applications are limited due to some potential complications including long term immunosuppressant, risk of causing limbal stem cell deficiency in the healthy contralateral eye[1,3].

Platelet-rich plasma (PRP) has become a common treatment in the field of ophthalmological surgery, plastic reconstructive surgery, trauma and skin burns[4]. PRP is a nontoxic and nonimmunogenic blood component obtained by centrifuging whole blood to get a cellular constitute of platelet-enriched plasma. PRP contains several growth factors, including insulin-like growth factors 1 and 2, transforming growth factor, hepatocyte growth factor, fibroblast growth factor, and vascular endothelial growth factor. Besides, it includes bioactive factors or non-growth factors; serotonin, histamine, dopamine, calcium, adenosine, fibronectin, fibrin, and vitronectin. These factors have been suggested to accelerate epithelial and endothelial regeneration, provoke angiogenesis and cell differentiation, enhance the hemostatic response, increase

 DOI: 10.21608/ejh.2019.7018.1059

collagen synthesis and assist cell migration, thus stimulate soft tissue healing[4,5].

It has been proposed that PRP can be used for subconjunctival application revealing an acceleration and improvement in corneal epithelial wound healing[6].

The aim of this study was to evaluate and compare the alleviating effect of a single-shot subconjunctival PRP injection applied either after 2 hours or 48 hours on an alkali-induced corneal burn.

MATERIAL AND METHODS

Thirty adult male albino rats weighing 150–180 grams each were used in this study. They were kept on a standard 12h-light/12h-dark cycle before the experiment and throughout the study period. The rats were kept in clean properly ventilated cages with free access to a balanced laboratory diet and water. They underwent acclimatization for 2 weeks before the experiment. The experiment was approved by the Local Ethics Committee of Faculty of Medicine, Tanta University, Egypt.

The animals were randomly allocated into five equal groups

Group I (control group): was subdivided into two equal subgroups; subgroup (Ia) were left untreated, subgroup (Ib) received a single subconjunctival injection of 0.5 ml of phosphate buffered saline (PBS) then left untreated for the rest of the experiment (10 days).

Group II (PRP-treated group): Rats of this group received a single subconjunctival injection of 0.5 ml of platelet-rich plasma (PRP) then were left untreated for the rest of the experiment (10 days). PRP was prepared as previously described; briefly, intra-cardiac blood sample was aspirated from the rats on citrate dextrose anticoagulant under general anesthesia. The whole blood was centrifuged at 3000 rpm for 7 minutes at 20°C to sediment down red blood cells (RBCs). The supernatant plasma was aspirated and centrifuged for another round at 4000 rpm for 5 minutes at 20°C to pellet down the platelets (PRP)[7].

Group III (Alkali burn group): Rats of this group were anesthetized by intramuscular injection of 0.5mg/kg ketamine, then a filter paper soaked in 1 M NaoH was applied on the center of cornea of right eyes only for 25 seconds then was rinsed with 10 ml of distilled water[8]. The left eyes were left to enable the animals to move, eat and drink. The animals were left untreated for the rest of the experiment (10 days after the alkali burn). NaOH was obtained from ElGomhoria chemicals company (Cairo, Egypt) in the form of white powder.

Group IV (Alkali burn +PRP after 2 hours): Alkali burn was inflected on the rats of this group as described in group III, then received a single subconjunctival injection of 0.5 ml of platelet-rich plasma (PRP) after 2 hours of the burn and were left untreated for the rest of the experiment (10 days after the alkali burn).

Group V (Alkali burn +PRP after 48 hours): Alkali burn was inflected on the rats of this group as described in group III, then received a single subconjunctival injection of 0.5 ml of platelet-rich plasma (PRP) after 48 hours of the burn and were left untreated for the rest of the experiment (10 days after the alkali burn).

On the 10th day of the alkali burn, all animals were euthanized under intraperitoneal injection of pentobarbital (40 mg/kg)[9]. Corneas were dissected out and processed for light microscopy.

For light microscopic examination

Specimens were immersed in 10% neutral-buffered formalin, washed, dehydrated, cleared and embedded in paraffin. Sections of 5µm thickness were stained with hematoxylin and eosin (H&E) and Periodic Acid Schiff reagent (PAS) for detection of mucopolysaccharides[10].

For immunohistochemistry

Five µm thick sections were dewaxed, rehydrated, and washed with phosphate buffered saline (PBS). The sections were then incubated overnight in a humid chamber with the primary antibody at 4°C; rabbit polyclonal anti-P53 (ab131442; Abcam, Massachusetts, USA) for detection of apoptosis, rabbit polyclonal anti-Ki67 (ab15580; Abcam, Massachusetts, USA) for detection of cell proliferation, rabbit polyclonal anti-MMP1 (ab137332; Abcam, Massachusetts, USA) and rabbit monoclonal anti-MMP9 (ab76003; Abcam, Massachusetts, USA), both for detection of matrix alterations. The sections were then rinsed three times in PBS and incubated with the corresponding biotinylated secondary antibody for one hour at room temperature. Streptavidin peroxidase was then added for 10 minutes and rinsed again three times in PBS. Immunoreactivity was visualized using 3,3'diaminobenzidine (DAB)-hydrogen peroxide as a chromogen. Sections were counterstained with Mayer's hematoxylin. The negative control sections were prepared by excluding the primary antibodies[11]. The positive controls of the primary antibodies were rat colon tissue, mouse spleen tissue, mouse prostate tissue and human spleen tissue respectively.

Morphometric study

The images were analyzed using Leica Qwin 500 C Image analyzer computer system (Leica Imaging System LTD., Cambridge, England) at (Central Research Lab, Faculty of Medicine, Tanta University, Egypt). Ten different non-overlapping randomly-selected fields from each slide at a magnification of 400 were quantified for:

1. Mean corneal epithelial thickness in H&E-stained sections.
2. Mean Descemet's membrane thickness (µm) in PAS-stained sections.
3. Mean color intensity of P53-immunohistochemical positive reaction in DAB-stained sections.

4. Mean percentage (%) of Ki67-immunohistochemical positive cells in DAB-stained sections.
5. Mean area percentage (%) of MMP1 and MMP9-immunohistochemical positive reaction in DAB-stained sections.

Statistical analysis

The data were analyzed by using one-way analysis of variance (ANOVA) followed by Tukey's test for comparison between the groups using statistical package for social sciences statistical analysis software (IBM SPSS Statistics for Windows, IBM Corp, Version 22.0. Armonk, NY, USA). All values were expressed as mean ± standard deviation. Differences were regarded as significant if probability value $p<0.05$ and highly significant if $p<0.001$[12].

RESULTS

Histological findings

H&E staining

Group I (Control) and PRP-treated rats (Group II)

Corneal sections from control rats (Group I) and PRP-treated rats (Group II) revealed the characteristic histological structure of cornea, where it was composed of three distinct layers; the outer epithelium, the inner endothelium, and the intermediate stroma. The corneal epithelium was a non-keratinized stratified squamous epithelium consisting of a single basal layer of columnar cells and 2-3 layers of intermediate polygonal (wing) cells covered with 1-2 layers of superficial flattened squamous cells. The epithelium was supported by Bowman's membrane. The stroma was composed of parallel lamellae of regular dense acidophilic collagenous fibres forming the main bulk of the cornea. Keratocytes were flattened cells scattered in the ground substance between the stromal lamellae. The inner endothelium of the cornea was composed of single layer of flattened cells supported by a thick homogenous Descemet's membrane (Figure 1).

Group III (Non-treated Alkali burned Cornea, 10 days after the alkali burn)

Corneal sections from alkali-burn group depicted corneal epithelium with focal discontinuity and denudation, while other parts revealed focal disorganization and stratification. Moreover, the corneal epithelium showed vacuolated cytoplasm and some hyperchromatic, pyknotic and karyolytic nuclei. The Bowman's membrane appeared irregular with focal disruption in some areas. The underlying stroma showed extensive separation of collagen lamellae with wide spaces in between. keratocytes were large and irregularly dispersed in between the lamellae. The Descemet's membrane was apparently thinned out and disrupted in some areas. Mononuclear cellular infiltration and invasion with small blood vessels could be observed in between the irregularly dispersed collagen fibers of the stroma (Figures 2, 3, 4).

Group IV (Alkali burn+PRP after 2 hours)

Corneal specimens revealed a near normal corneal histological structure with intact epithelium, yet some epithelial cells with vacuolated cytoplasm could be detected. The Bowman's membrane appeared intact. The stroma showed organized collagenous fibers with few spaces in between. Organized flattened keratocytes were scattered in the stroma. The Descemet's membrane and the endothelium were apparently regular and continuous (Figure 5).

Group V (Alkali burn+PRP after 48 hours)

Corneal specimens revealed a disturbed corneal histological structure with vacuolated epithelium and some nuclear changes in the form of hyperchromatic, pyknotic and karyolytic nuclei. A focal discontinuity and irregularity of the outer surface could be observed. The Bowman's membrane was undistinguished from the underlying stroma which showed some disorganized keratocytes. The stroma depicted some unorganized collagenous fibers with some spaces in between. The Descemet's membrane was intact, but the endothelium showed some disruption (Figure 6).

PAS histochemical staining

PAS-stained corneal sections from control group revealed a strong positive PAS reaction in the Descemet's membrane with a characteristic magenta red coloration (Figure 7). While sections from alkali burn (group III) showed a weak positive PAS reaction in the Descemet's membrane which appeared thinned out with focal disruption (Figure 8). On the other hand, sections from group IV showed an apparently strong positive PAS reaction in the Descemet's membrane (Figure 9). Whereas sections from group V depicted a moderate positive PAS reaction in the Descemet's membrane (Figure 10).

Morphometrical analysis of the mean color intensity of PAS positive reaction and the mean thickness of the Descemet's membrane revealed a highly significant decrease in the group III (12.98±1.76, 3.78±1.01 respectively) compared to the control (20.98±2.22, 6.09±0.98 respectively), while a non-significant difference was recorded between group IV (17.98±3.99, 5.49±0.99 respectively) and control group. On the other hand, group V showed a significant decrease (15.90±3.97, 4.04±1.81 respectively) compared to the control (Table 1, Histogram 1A, B).

Immunohistochemical staining

Immunohistochemical results for P53

Sections from control group revealed a faint positive cytoplasmic immunoreaction for p53 strictly in corneal epithelial cells in the form of a brownish coloration (Figure11). While sections from alkali burn [group III] showed a strong positive immunoreaction (Figure 12). On the other hand, sections from group IV showed a moderate positive immunoreaction in the corneal epithelial cells (Figure 13). Yet sections from group V depicted a moderate to strong positive immunoreaction (Figure 14).

Morphometrical analysis of the mean color intensity of p53 immunohistochemical reaction revealed a highly significant increase in the group III (46.89±3.88) compared to the control (21.47±1.9), while a non-significant difference was recorded between group IV (23.98±3.54) and control group. On the other hand, group V showed a significant increase (28.33±6.11) compared to the control (Table 1, Histogram 1C).

Immunohistochemical results for Ki67

Sections from control group showed few cells with positive nuclear Ki67 immunoexpression in the basal layer of the corneal epithelium in the form of a brownish coloration (Figure 15). While sections from alkali burn group III depicted numerous Ki67-immunopositive cells in the basal and supra-basal layers of the corneal epithelium (Figure 16). On the other hand, sections from group IV revealed some Ki67-immunopositive cells in the basal and supra-basal layers of the corneal epithelium (Figure 17). Nevertheless, sections from group V showed many Ki67-immunopositive cells in the basal and supra-basal layers of the corneal epithelium (Figure 18).

Morphometrical analysis of the mean percentage of Ki67-immunopositive cells revealed a highly significant increase in the group III (19.91±1.31) compared to the control (6.96±0.93), while a non-significant difference was recorded between group IV (8.21±2.48) and control group. On the other hand, group V showed a significant increase (10.23±2.88) compared to the control (Table 1, Histogram 1D).

Immunohistochemical results for MMP-1

Sections from control group showed a weak positive cytoplasmic expression for MMP-1 in the form of a brownish coloration in the interstitial space of the basal epithelial cells restricted to the basal region of the corneal epithelium (Figure 19). Whereas sections from alkali burn group III revealed an extensive strong positive expression for MMP-1 both in the interstitial space of the basal and supra-basal epithelial cells and in the corneal stroma (Figure 20). On the other hand, sections from group IV depicted a moderate MMP-1 immunopositive reaction in the interstitial space of the basal epithelial cells (Figure 21). Yet, section from group V showed a strong MMP-1 immunopositive reaction in the interstitial space of basal and some supra-basal epithelial cells of the corneal epithelium (Figure 22).

Morphometrical analysis of the mean area percentage of MMP1-immunopositive reaction revealed a highly significant increase in the group III (15.65±3.66) compared to the control (5.87±0.51), while a non-significant difference was recorded between group IV (7.02±1.88) and control group. On the other hand, group V showed a significant increase (9.09±3.03) compared to the control (Table 1, Histogram 1E).

Immunohistochemical results for MMP-9

Sections from control group revealed a weak cytoplasmic localization of MMP-9 immunopositive expression in the basal and supra-basal epithelial cells in the form of a brownish coloration (Figure 23). Whereas sections from alkali burn group III revealed an extensive strong positive expression for MMP-9 in the basal and supra-basal epithelial cells (Figure 24). On the other hand, sections from group IV depicted a moderate MMP-9 immunopositive reaction in the basal and some supra-basal epithelial cells (Figure 25). Additionally, section from group V showed a moderate to strong MMP-9 immunopositive reaction in basal and some supra-basal epithelial cells of the corneal epithelium (Figure 26).

Morphometrical analysis of the mean area percentage of MMP-9 immunopositive reaction revealed a highly significant increase in the group III (13.96±2.11) compared to the control (7.22±1.83), while a non-significant difference was recorded between group IV (7.88±1.65) and control group. On the other hand, group V showed a significant increase (9.06±1.01) compared to the control (Table 1, Histogram 1F).

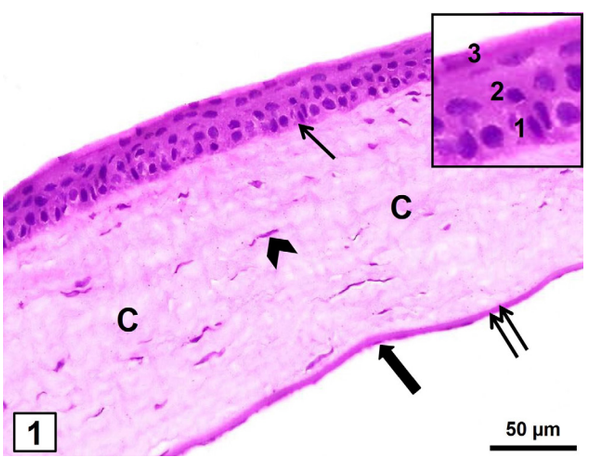

Fig. 1: A photomicrograph from the rat cornea of the control group showing the corneal epithelium composed of a single basal layer of columnar cells (1) and intermediate polygonal cells (2) covered with superficial flattened cells (3). The epithelium is supported by Bowman's membrane (arrow). The stroma contains parallel lamellae of regular dense acidophilic collagenous fibres (C) with keratocytes (arrow head) scattered in between the stromal lamellae. The inner endothelium is a single layer of flattened cells (thick arrow) supported by Descemet's membrane (double arrow). (H&E X400, scale bar= 50µm, inset X1000)

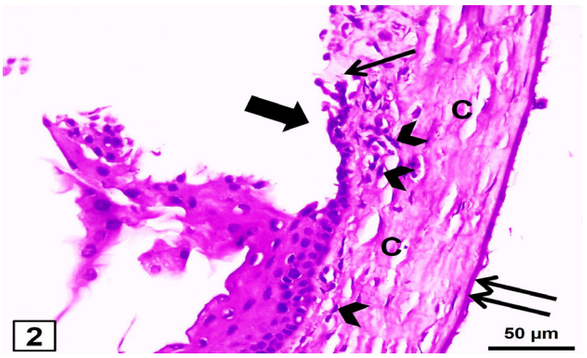

Fig. 2: A photomicrograph from the rat cornea of the alkali burn group showing corneal epithelium with focal discontinuity and denudation (thick arrow). The Bowman's membrane appears irregular with focal disruption in some areas (thin arrow). The underlying stroma shows extensive separation of collagen lamellae with wide spaces in between (C). Notice large irregularly dispersed keratocytes (arrow heads) in between the lamellae. The Descemet's membrane appears thinned out (double thin arrows). (H&E x400, scale bar= 50µm)

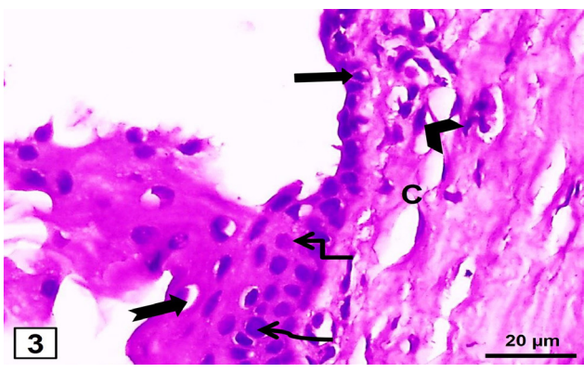

Fig. 3: A higher magnification photomicrograph from the rat cornea of the alkali burn group showing vacuolated cytoplasm (notched arrow) and some hyperchromatic (wavy arrow), pyknotic (thick arrow) and karyolytic (angular arrow) nuclei. Notice large irregularly dispersed keratocytes (arrow head) in between the widely separated lamellae (C). (H&E x1000, scale bar= 20µm)

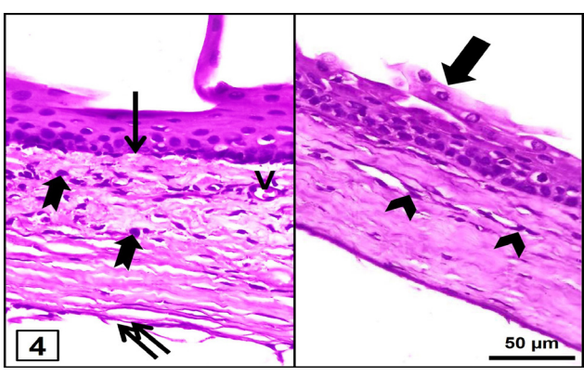

Fig. 4: A photomicrograph from the rat cornea of the alkali burn group showing corneal epithelium with focal disorganization and stratification (thick arrow). The Bowman's membrane appears irregular with focal disruption in some areas (thin arrow). The underlying stroma shows mononuclear cellular infiltration (notched arrows) and invasion with small blood vessels (V) in between the irregularly dispersed collagen fibers. Notice large irregularly dispersed keratocytes (arrow heads) in between the lamellae. The Descemet's membrane appears thinned out and disrupted in some areas (double thin arrows). (H&E x400, scale bar= 50µm)

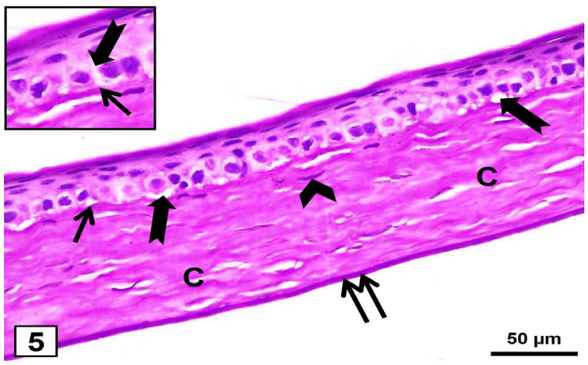

Fig. 5: A photomicrograph from the rat cornea of the alkali burn and PRP after 2 hours group showing a near normal corneal histological structure with intact epithelium with few epithelial cells showing vacuolated cytoplasm (notched arrows). The Bowman's membrane appears intact (thin arrows). The stroma shows organized collagenous fibers with few spaces in between (C). Organized flattened keratocytes (arrow head) are scattered in the stroma. The Descemet's membrane and the endothelium appears regular and continuous (double thin arrows). (H&E x400, scale bar= 50µm, inset x1000)

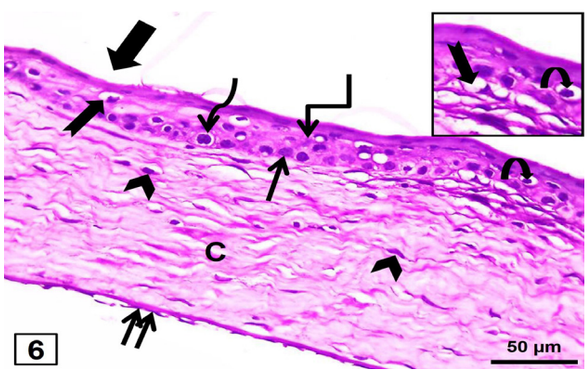

Fig. 6: A photomicrograph from the rat cornea of the alkali burn and PRP after 48 hours group showing a disturbed corneal histological structure with vacuolated epithelium (notched arrow) and many nuclear changes in the form of hyperchromatic (wavy arrow), pyknotic (curved arrow) and karyolytic (angular arrow) nuclei. A focal discontinuity and irregularity of the outer surface is observed (thick arrow). The Bowman's membrane is undistinguished from the underlying stroma which shows some disorganized keratocytes (arrow heads). The stroma shows some unorganized collagenous fibers with some spaces inbetween (C). The Descemet's membrane is continuous but the endothelium shows some disruption (double thin arrows). (H&E x400, scale bar= 50µm, inset x1000)

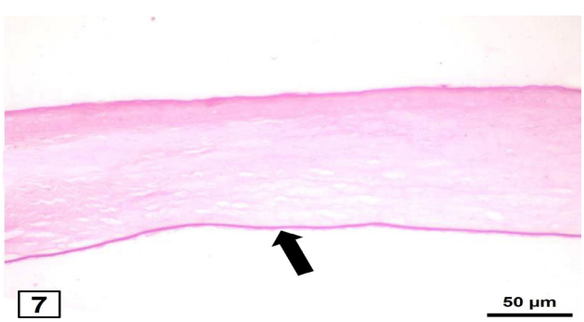

Fig. 7: A photomicrograph from the rat cornea of control group showing a strong positive PAS reaction in the Descemet's membrane (thick arrow) with a characteristic magenta red coloration (PAS x400, scale bar= 50µm)

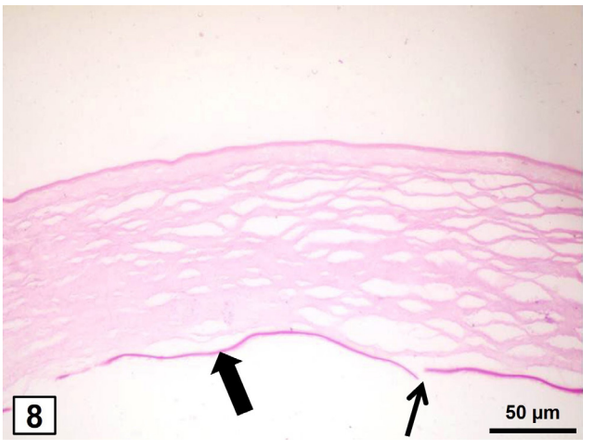

Fig. 8: A photomicrograph from the rat cornea of alkali burn group showing a weak positive PAS reaction in the Descemet's membrane (thick arrow) with focal disruption (thin arrow) (PAS x400, scale bar= 50µm)

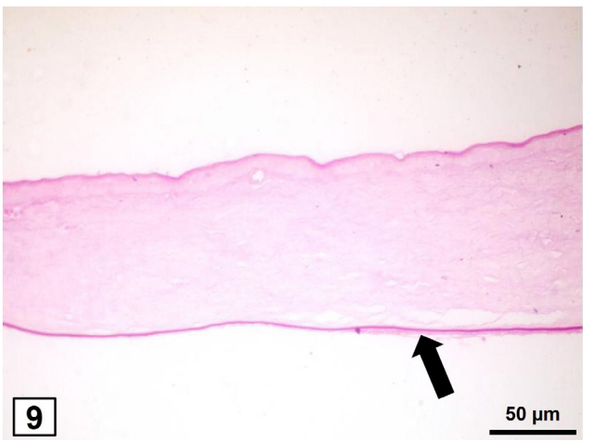

Fig. 9: A photomicrograph from the rat cornea of alkali burn and PRP after 2 hours group showing a strong positive PAS reaction in the Descemet's membrane (thick arrow) (PAS x400, scale bar= 50µm)

Fig. 10: A photomicrograph from the rat cornea of alkali burn and PRP after 48 hours group showing a moderate positive PAS reaction in the Descemet's membrane (thick arrow) (PAS x400, scale bar= 50µm)

Fig. 11: A photomicrograph from the rat cornea of control group I showing a faint positive cytoplasmic immunoreaction for p53 strictly in corneal epithelial cells in the form of brownish coloration (arrow) (P53 x400. scale bar= 50µm)

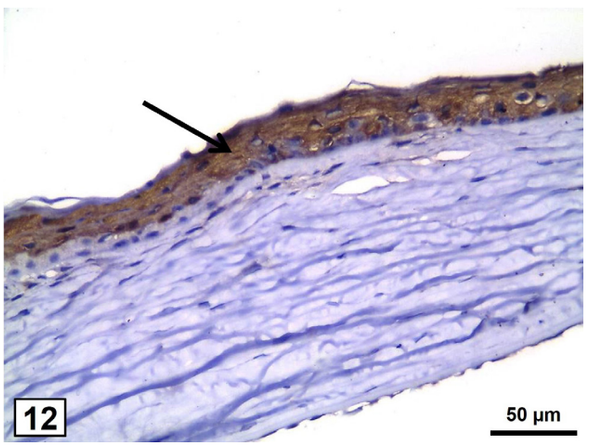

Fig. 12: A photomicrograph from the rat cornea of group III showing a strong positive immunoreaction for p53 in corneal epithelial cells (arrow) (P53 x400, scale bar= 50µm)

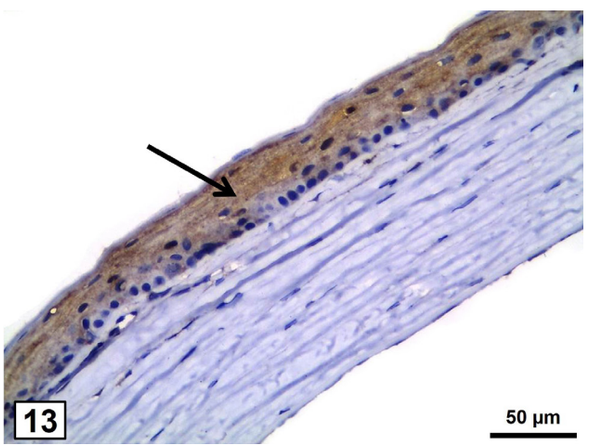

Fig. 13: A photomicrograph from the rat cornea of group IV showing a moderate positive immunoreaction for p53 in corneal epithelial cells (arrow) (P53 x400, scale bar= 50µm)

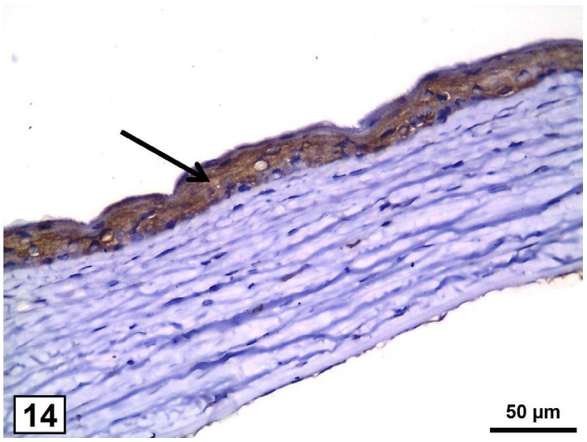

Fig. 14: A photomicrograph from the rat cornea of group V showing a strong positive immunoreaction for p53 in corneal epithelial cells (arrow) (P53 x400, scale bar= 50µm)

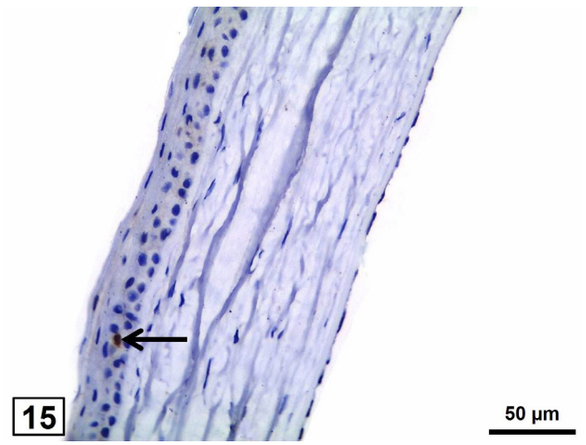

Fig. 15: A photomicrograph from the rat cornea of control group I showing few nuclear Ki67-immunopositive cells (arrow) with a brownish nuclear coloration (Ki67 x400, scale bar= 50µm)

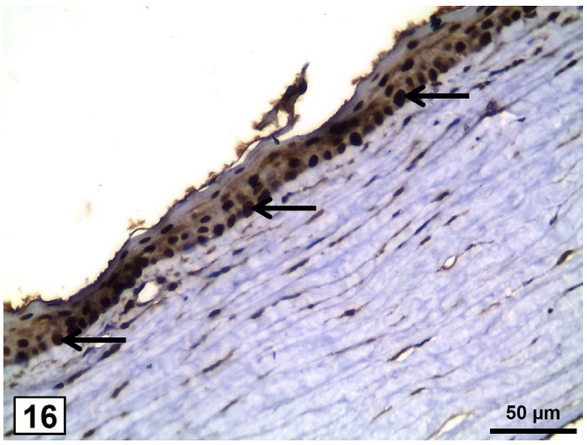

Fig. 16: A photomicrograph from the rat cornea of group III showing numerous Ki67-immunopositive cells (arrows) (Ki67 x400, scale bar= 50µm)

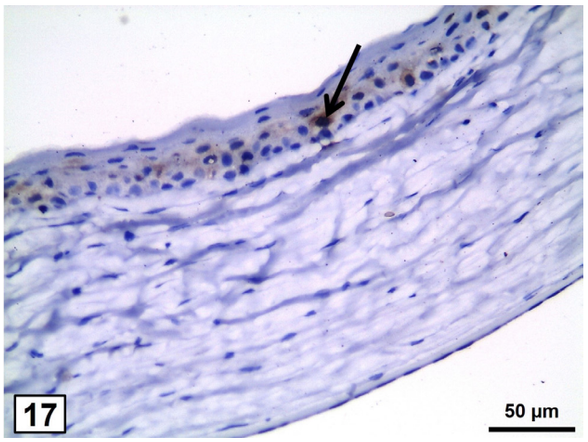

Fig. 17: A photomicrograph from the rat cornea of group IV showing some Ki67-immunopositive cells (arrow) (Ki67 x400, scale bar= 50µm)

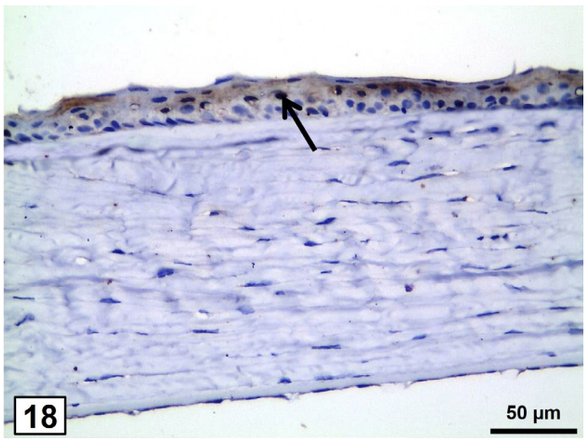

Fig. 18: A photomicrograph from the rat cornea of group V showing many Ki67-immunopositive cells (arrow) (Ki67 x400, scale bar= 50µm)

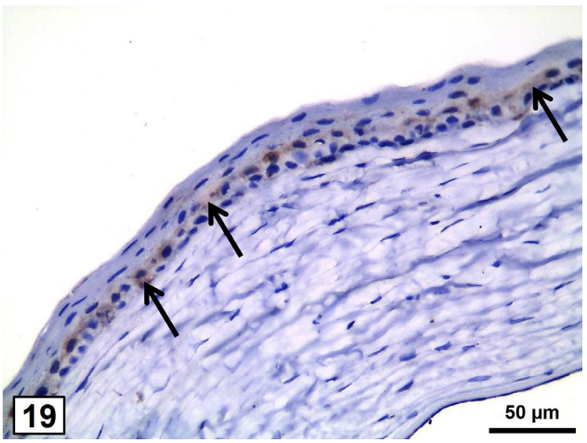

Fig. 19: A photomicrograph from the rat cornea of control group I showing weak cytoplasmic positive MMP-1 immunoreaction in the interstitial space of the basal epithelial cells restricted to the basal region of the corneal epithelium in the form of brownish nuclear coloration (arrows) (MMP-1 x400, scale bar= 50µm)

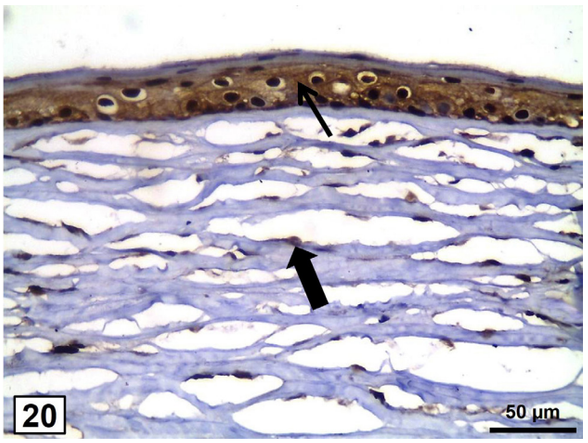

Fig. 20: A photomicrograph from the rat cornea of group III showing extensive strong positive MMP-1 immunoreaction in the interstitial space of the basal and supra-basal epithelial cells (thin arrow) and the corneal stroma (thick arrow) (MMP-1 x400, scale bar= 50µm)

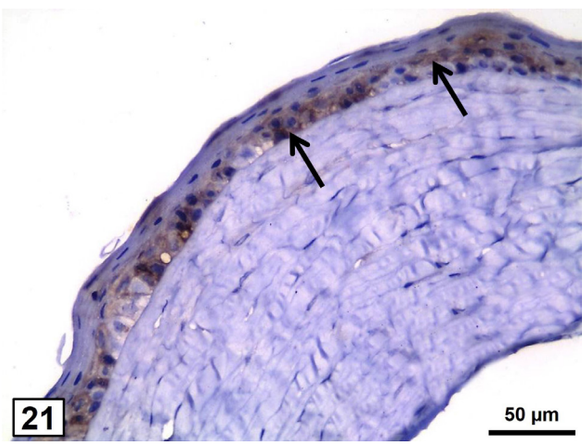

Fig. 21: A photomicrograph from the rat cornea of group IV showing moderate positive MMP-1 immunoreaction in the interstitial space of the basal epithelial cells (arrows) (MMP-1 x400, scale bar= 50µm)

Fig. 22: A photomicrograph from the rat cornea of group V showing strong positive MMP-1 immunoreaction in the interstitial space of the basal and some supra-basal epithelial cells (arrows) (MMP-1 x400, scale bar= 50µm)

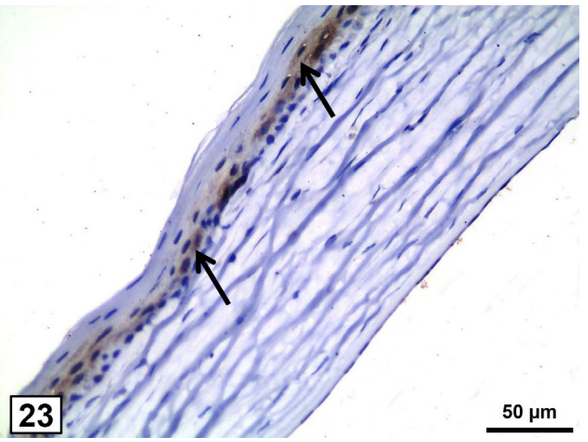

Fig. 23: A photomicrograph from the rat cornea of control group I showing weak cytoplasmic positive MMP-9 immunoreaction in cytoplasm of the basal and supra-basal epithelial cells in the form of brownish nuclear coloration (arrows) (MMP-9 x400, scale bar= 50µm)

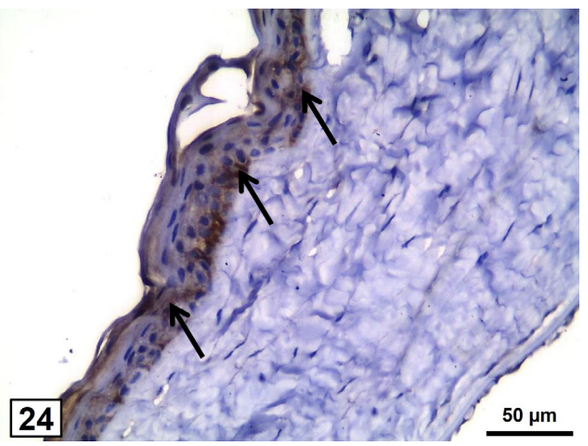

Fig. 24: A photomicrograph from the rat cornea of group III showing extensive strong positive MMP-9 immunoreaction in the basal and supra-basal epithelial cells (arrows) (MMP-9 x400, scale bar= 50µm)

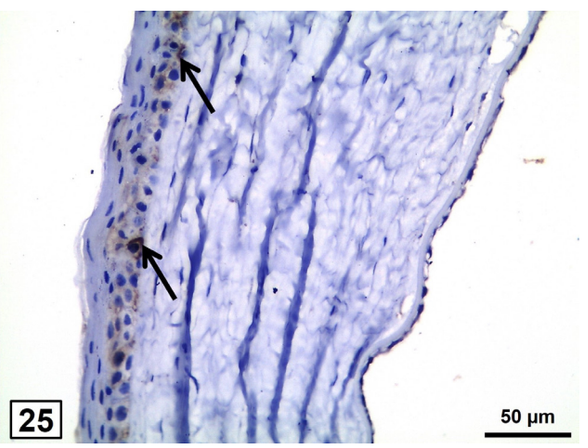

Fig. 25: A photomicrograph from the rat cornea of group IV showing moderate positive MMP-9 immunoreaction in the basal and supra-basal epithelial cells (arrows) (MMP-9 x400, scale bar= 50µm)

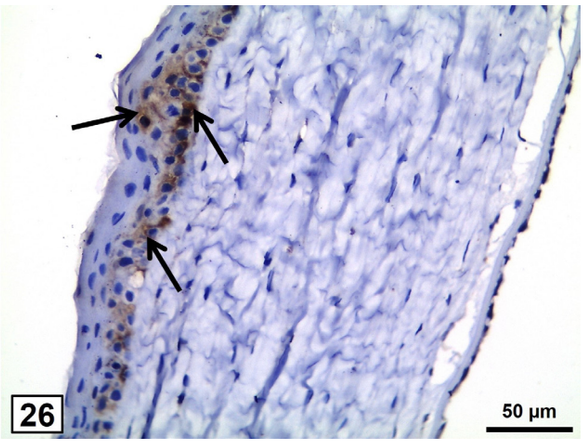

Fig. 26: A photomicrograph from the rat cornea of group V showing moderate to strong positive MMP-9 immunoreaction in the basal and some supra-basal epithelial cells (arrow) (MMP-9 x400, scale bar= 50µm)

Table 1: Morphometric and statistical analysis of different morphometric parameters of all groups

Parameters	Group I	Group II	Group III	Group IV	Group V
Mean color intensity of PAS positive reaction	20.98±2.22	21.90±1.76	12.98±1.76**	17.98±3.99	15.90±3.97*
Mean thickness of Descemet's membrane (µm)	6.09±0.98	6.79±0.81	3.78±1.01**	5.49±0.99	4.04±1.81*
Mean color intensity of p53-immunopositive reaction	21.47±1.9	21.06±1.2	46.89±3.88**	23.98±3.54	28.33±6.11*
Mean percentage of Ki67-immunopositive cells	6.96±0.93	6.01±0.27	19.91±1.31**	8.21±2.48	10.23±2.88*
Mean area percentage of MMP-1 immunopositive reaction	5.87±0.51	5.01±0.63	15.65±3.66**	7.02±1.88	9.09±3.03*
Mean area percentage of MMP-9 immunopositive reaction	7.22±1.83	7.09±1.09	13.96±2.11**	7.88±1.65	9.06±1.01*

Data is expressed as mean ± standard deviation. *indicates significant versus control, **indicates highly significant versus control

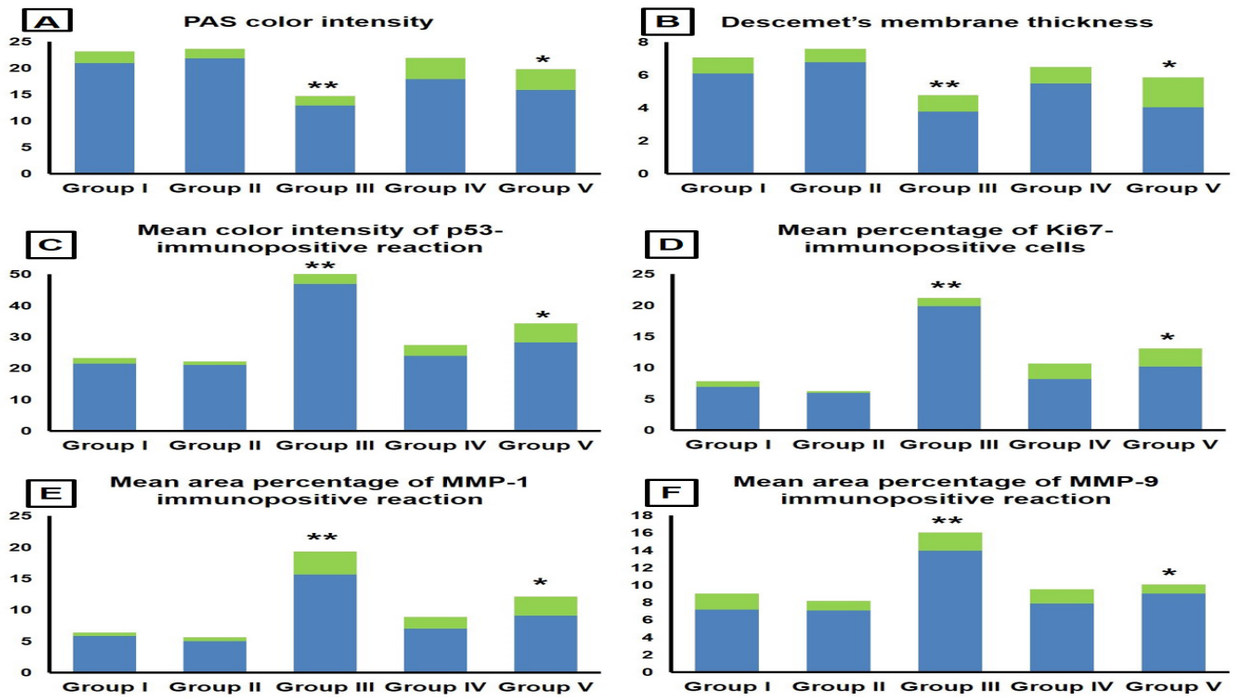

Histogram 1: Morphometrical and statistical analysis of the different study groups; A] Mean color intensity of PAS histochemical reaction, B] Mean thickness of Descemet's membrane(µm), C] Mean color intensity of P53-immunopositive reaction, D] Mean percentage of Ki-67 immunopositive cells, E] Mean area percentage of MMP-1 immunopositive reaction, F] Mean area percentage of MMP-9 immunopositive reaction. ** indicates highly significant vs control, * indicates significant vs control.

DISCUSSION

Corneal alkali burns are one of the most frequent traumas of the eye and have been considered as a true ocular emergency that requires immediate and intensive evaluation and treatment. The sequelae of corneal burn can be severe and challenging to manage, resulting in permanent visual impairment[1,13]. Therefore, the current study was designed to evaluate and compare the alleviating effect of a single-shot subconjunctival PRP injection applied either after 2 hours or 2 days of an alkali-induced corneal burn.

In the present work, focal epithelial discontinuity and denudation were noticed 2 days after application of NaOH on the center of rats' corneas, while other parts revealed focal disorganization and stratification. In addition, vacuolated epithelial cells with hyperchromatic, pyknotic and karyolytic nuclei were detected. Irregular focal disrupted Bowman's membranes were observed. Moreover, extensive separation of collagen lamellae with large irregularly dispersed keratocytes were observed in the underlying stroma. Additionally, mononuclear cellular infiltration and invasion with small blood vessels were observed in the stroma. The Descemet's membranes were apparently thinned out and disrupted in some areas. These findings coincided with those of a previous study[14], who reported conjunctival congestion, corneal epithelial defects, edema and neovascularization upon inducing corneal alkali burn grade II in a mouse model.

Researchers have related the burning effect of NaOH to the anion (hydroxyl) group that causes saponification of the fat and lipids, resulting in tissue softening, followed by increasing the penetration ability of the cation chemicals[15]. While other researchers[16,17] attributed the deleterious effect of alkali on cornea to its strong inflammatory reaction which is characterized by cell infiltration and production of proteolytic enzymes, cytokines oxidative derivatives that could cause severe loss of the extracellular matrix.

In the current work, corneal specimens treated by PRP after 2 hours of induction of the alkali burn showed a near normal histological structure. The epithelium became intact, but some cells had vacuolated cytoplasm. The Bowman's membrane appeared intact. Moreover, collagenous fibers of stroma were organized with few spaces in between. In addition, keratocytes appeared organized, flattened and scattered in the stroma. The Descemet's membranes and the endothelium were apparently regular and continuous.

Researchers have reported similar findings after using a single-dose of subconjunctival PRP injection to investigate its effect on corneal epithelial wound healing in a rabbit model[6]. They recorded epithelial regeneration after 10 days of treatment with minimal inflammation and typical fibroblast structure. Additionally, they related the repairing effect of PRP on corneal tissue to its content of a great number of platelets. They added that platelets could attach to the ocular surfaces and accelerate biochemical and biological mechanisms of healing.

Moreover, a previous report[18] argued that the platelets alpha-granules contained storage of growth factors, including platelet-derived growth factors, transforming growth factor β (TGF-β), epithelial growth factors, fibroblast growth factors, insulin-like growth factor I, and vascular endothelial growth factors, as well as cytokines, chemokines, and newly synthesized active metabolites. These products are involved in migration, differentiation and proliferation of corneal epithelial cells, thus helping to heal and maintain the proper condition of the ocular surface.

In this study, animal group treated by PRP after 48 hours from induction of alkali burn showed a disturbed histological structure with vacuolated epithelium and hyperchromatic, pyknotic and karyolytic nuclei. The outer surface revealed a focal discontinuity and irregularity. The Bowman's membranes appeared undistinguished from the underlying stroma. Moreover, some of the stromal collagenous fibers were unorganized with some spaces and disorganized keratocytes in between. The Descemet's membranes were intact but the endothelium showed some disruption. These findings were in line with a previous study[19], who tested the early and late phase (2 weeks post injury) effects of PRP injection into and around the damaged intervertebral disc. They reported that earlier intervention in severely degenerated discs would be more beneficial than delayed PRP treatment. They found that immediate PRP-treated discs maintenance had a better structure, cellularity, and hydration. In contrast to other researchers[20], who found no significant difference between immediate or delayed administration of PRP in contusion-injured gastrocnemius muscle.

Current results strongly suggested that early PRP intervention in alkali-injured cornea was more effective in alleviating corneal damage rather than delayed PRP treatment. It could be explained by PRP strong anti-inflammatory effect that could early antagonize the inflammatory effect of NaOH on corneal tissue. This was supported by the work of other researchers who suggested that PRP was not only a rich source of growth factors, but also contained antibacterial and fungicidal proteins, matrix metalloproteinases (MMPs), coagulation factors and membrane glycoproteins that modify inflammation through inducing the synthesis of other integrins, interleukins, chemokines, and cytokines[21]. Moreover, another study reported that PRP had reduced cellular inflammation markers like E-selectin, vascular cell adhesion molecule and human leukocyte antigen DR (HLA-DR). They also reported that PRP could act as an anti-inflammatory agent by producing endogenous anti-inflammatory factors and by affecting monocyte cytokine release[22].

In the present work, a highly significant decrease in PAS positive reaction in group III compared to the control was reported, while a non-significant difference was recorded between group IV and control group. On the other hand, group V showed a significant decrease compared to the control. These results were opposed by the finding of

a previous study[3], who reported an apparent increase in the thickness of the PAS positive Descemet's membrane of the cornea of rabbits of alkali burn subgroups compared to control group. The authors attributed the increase in the thickness of Descemet's membrane to the change in pH of the corneal endothelium leading to a decrease in the barrier effectiveness together with a decrease in the pump function.

P53 gene is a tumor-suppressor gene that plays a role in abnormal types of cell proliferation and apoptosis where it prevents the replication of genomes that have suffered from DNA damage[23]. P53 is synthesized in the cytoplasm and transported into the nucleus where it acts as a nuclear transcription factor that transactivates genes involved in apoptosis[24]. On the other hand, P53 induces apoptosis via a mitochondrial pathway in which p53 binds to the outer mitochondrial membrane, induces its permeabilization, and forms complexes with the protective Bcl XL and Bcl-2 proteins. The binding of p53 to these factors triggers cytochrome c release and caspase activation[25].

In this research, there was a significant up-regulation of p53 immunohistochemical cytoplasmic expression in alkali burn group III compared to the control, while a non-significant difference was recorded between group IV and control group. On the other hand, group V showed a significant increase compared to the control. The alkali-burn group p53 immune staining findings agreed with the results of other researchers[16], who observed corneal stromal melting after exposure to NaOH and recorded that stromal cells staining with TUNEL revealed apoptosis. Moreover, group IV p53 immune staining results were concordant with another study who found that immediate post-traumatic intra-articular injection of PRP had reduced impact-induced chondrocyte apoptosis in rabbits[26]. Additionally, researchers had previously reported a significant decrease in the number of apoptotic cells after co-culturing osteoarthritic chondrocytes with increasing concentrations of PRP[27]. They related that to PRP ability to induce a significant decrease in the expression of caspase 3 and Bad while significantly increasing Bcl2 expression. Another study[28] added that apoptosis could be inhibited by the epithelial growth factor (EGF).

Ki-67 is a nuclear protein expressed in all proliferating cells, and it is a widely used biomarker to estimate the proportion of dividing cells in grading of tumors[29]. In this work, immunohistochemical staining for Ki-67 was used to confirm the observed epithelial proliferation. A highly significant increase in Ki-67 expression was reported in group III compared to the control, while a non-significant difference was recorded between group IV and control group. On the other hand, group V showed a significant increase compared to the control. This came in agreement with the results of other researchers who reported a higher number of Ki-67 positive cells in the basal epithelial layers of cornea burned with silver nitrate[13]. They suggested that the epithelial cell renewal was dependent on basal cell mitotic activity. They added that these proliferating cells were initially derived from quiescent stem cells in the limbal periphery, which were activated by injury to become proliferative.

On the other hand, results from both PRP-treated groups could be explained by the findings of another study which suggested that TGF-β1 and PDGF in PRP stimulated proliferation of mesenchymal cells[30]. Other researchers[31] indicated that PRP inhibited excessive collagen deposition, suggesting that treatment with PRP may decrease the progression of fibrosis in damaged endometrium. Moreover, another work had reported prevention of contusion-injured skeletal muscle fibrosis treated by combination of PRP injection and oral losartan[32]. They claimed that this combination could enhance muscle healing by stimulating muscle regeneration and angiogenesis.

MMPs are calcium-dependent zinc-containing endopeptidases, secreted by keratocytes, epithelial cells. MMPs participate in and promote corneal inflammation. MMP-1 is associated with corneal destruction after injury and alkali-induced burns. While, MMP-9 digests denatured collagen, gelatin, and native type IV, V, and VII collagens as well as other extracellular components. Moreover, MMP-9 might be an important enhancing factor for inflammation preventing re-epithelialization of the cornea following thermal injury. However, the mechanism is still not well understood[33,34,35].

In the current study, MMP1 and MMP-9 immunopositive reactions showed a highly significant increase in the group III compared to the control group, while a non-significant difference was recorded between group IV and control group. On the other hand, group V showed a significant increase compared to the control group. This came in accordance with the work of other researchers in which MMP-1 and MMP-9 were detected in the basal membrane and superficial stroma after lamellar keratectomy[35]. The authors reported that the overexpression of MMP-1 and MMP-9 occurred in corneal ulcers and led to a rapid degradation of corneal extracellular matrix. On the other hand, current findings of PRP-treated groups were in accordance with the findings of another study which recorded MMP-1 downregulation in post-burn skin tissue after its treatment with mesenchymal stem cells pretreated with PRP[36]. This could be explained by the work of other researchers who found that MMP-9 was totally inhibited by endogenous MMP inhibitor present in PRP which binds MMPs and led to their clearance by endocytosis[37].

Taken altogether, it could be concluded from the findings of the current study that a single-shot subconjunctival PRP injection had an effective alleviating effect on alkali-induced corneal burn, yet the PRP injection after 2 hours of the burn was more efficient in restoring the corneal healthy surface rather than its application after 48 hours judging by different histological, histochemical, immunohistochemical and morphometrical techniques. Therefore, it is recommended to apply PRP as soon as the corneal burn happens, and that PRP application after 48 hours is not as promising as the earlier application.

CONFLICTS OF INTEREST

The authors have no conflicts of interest to declare.

REFERENCES

1. Singh P, Tyagi M, Kumar Y, Gupta KK, Sharma PD. 2013. Ocular chemical injuries and their management. Oman J Ophthalmol. 6(2): 83–86.
2. Acosta L, Castro M, Fernandez M, Oliveres E, Gomez-Demmel E, Tartara L. 2014. Treatment of corneal ulcers with platelet rich plasma. Arch Soc Esp Oftalmol. 89(2):48-52.
3. Ahmed SK, Soliman AA, Omar SMM, Mohammed WR. 2015. Bone Marrow Mesenchymal Stem Cell Transplantation in a Rabbit Corneal Alkali Burn Model (A Histological and Immune Histo-chemical Study). Int J Stem Cells. 8(1): 69–78.
4. Girgin M, Binnetoglu K, Duman K, Kanat BH, Cetinkaya Z, Ayten R, Ilhan YS, Ilhan N, Seker I, Timurkaan N. 2016. Effects of platelet rich plasma on fascial healing in rats with fecal peritonitis. Acta Cir Bras. 31(5):314-319.
5. Çirci E, Akman YE, Şükür E, Bozkurt ER, Tüzüner T, Öztürkmen Y. 2016. Impact of platelet-rich plasma injection timing on healing of Achilles tendon injury in a rat model. Acta Orthop Traumatol Turc. 50(3):366-72.
6. Tanidir ST, Yuksel N, Altintas O, Yildiz DK, Sener E, Caglar Y. 2010 The effect of subconjunctival platelet-rich plasma on corneal epithelial wound healing. Cornea. 29(6):664-669.
7. Ariede JR, Pardini MIC, Silva GF, Grotto RMT. 2015. Platelets can be a biological compartment for the Hepatitis C Virus. Brazilian Journal of Microbiology 46(2), 627-629
8. Khaksar E., Aldavood S. J., Abedi G. R., Sedaghat R., Nekoui O., Zamani-Ahmadmahmudi M. The effect of sub-conjunctival platelet-rich plasma in combination with topical acetylcysteine on corneal alkali burn ulcer in rabbits. Comp Clin Pathol (2013) 22:107–112
9. Gaertner, D.J., Hallman, T.M., Hankenson, F.C., Batchelder, M.A., 2008. Anesthesia and analgesia for laboratory rodents. In: Fish, R.E., Danneman, P.J., Brown, M., Karas, A.Z. (Eds.), Anesthesia and Analgesia in Laboratory Animals. , 2nd ed. Academic Press, London (UK), pp. 239–297.
10. Bancroft JD and Gamble M. Theory and Practice of Histological Techniques. sixth ed. Philadelphia: Churchill Livingstone: Elsevier; 2008. p. 126–127.
11. Buchwalow, I.B., Böcker, W., 2010. Immunohistochemistry: Basics and Methods. Springer, Heidelberg, Dordecht, London, New York, pp. 31–39.
12. Dawson-Saunders B, Trapp R. Basic and Clinical Biostatistics. third ed. Lange Medical Book/ McGraw-Hill Medical Publishing Division; 2001. p. 161–218.
13. Martin LF, Rocha EM, Garcia SB, Paula JS. 2013. Topical Brazilian propolis improves corneal wound healing and inflammation in rats following alkali burns. BMC Complement Altern Med. 13: 337.
14. Bai JQ, Qin HF, Zhao SH, 2016. Research on mouse model of grade II corneal alkali burn. Int J Ophthalmol. 9 (4):487-490.
15. Mashige k. 2015. Chemical and thermal ocular burns: a review of causes, clinical features and management protocol. South African Family Practice. 58(1): 1-4.
16. He J, Bazan NG, Bazan HE. 2006. Alkali-induced corneal stromal melting prevention by a novel platelet-activating factor receptor antagonist. Arch Ophthalmol. 124(1):70-78.
17. Lee KJ, Lee JY, Lee SH, Choi TH. 2013. Accelerating repaired basement membrane after bevacizumab treatment on alkali-burned mouse cornea. BMB Rep.46(4):195-200.
18. Alio JL, Rodriguez AE, Abdelghany AA, Oliveira RF. 2017. Autologous Platelet-Rich Plasma Eye Drops for the Treatment of Post-LASIK Chronic Ocular Surface Syndrome. J Ophthalmol. 2017:2457620.
19. Gullung GB, Woodall JW, Tucci MA, James J, Black DA, McGuire, RA. 2011. Platelet-rich plasma effects on degenerative disc disease: analysis of histology and imaging in an animal model. Evid Based Spine Care J. 2(4):13-18.
20. Delos D, Leineweber M, Chaudhury S, Alzoobaee S, Gao Y, Rodeo, SA. 2013. The Effect of Immediate and Delayed Injection of Platelet-Rich Plasma (PRP) on Muscle Contusion Healing in the Rat. BMB Rep. 46(4): 195–200.
21. Martini L, Via AG, Fossati C, Randelli F, Randelli P, Cucchi D. 2017. Single Platelet-Rich Plasma Injection for Early Stage of Osteoarthritis of the Knee. Joints. 5 (1):2-6.
22. Mazzocca AD, McCarthy MB, Intravia J, Beitzel K, Apostolakos J, Cote MP, Bradley J, Arciero RA. 2013. An in vitro evaluation of the anti-inflammatory effects of platelet-rich plasma, ketorolac, and methylprednisolone. Arthroscopy. 29(4):675-683.

23. Leigh-Brown S, Enriquez JA and Odom DT. 2010. Nuclear transcription factors in mammalian mitochondria. Genome Biol. 11(7): 215.

24. O'Brate A and Giannakakou P. 2003. The importance of p53 location: nuclear or cytoplasmic zip code? Drug Resist Update. 6(6): 313-322.

25. Vaseva AV and Moll UM. 2009. The mitochondrial p53 pathway Biochim Biophys Acta. 1787(5): 414.

26. de Rezende MU, da Silva RBB, Bassit ACF, Tatsui NH, Sadigursky D, Neto RB. 2011. Effect of Platelet-Rich Plasma on. impact-induced chondrocyte apoptosis Acta ortop. bras. 19 (2): 102-105.

27. Moussa M, Lajeunesse D, Hilal G, El Atat O, Haykal G, Serhal R, Chalhoub A, Khalil C, Alaaeddine N. 2017. Platelet rich plasma (PRP) induces chondroprotection via increasing autophagy, anti-inflammatory markers, and decreasing apoptosis in human osteoarthritic cartilage. Exp Cell Res. 352(1):146-156.

28. Wu TE, Chen CJ, Hu CC, Cheng CK. 2015. Easy-to-prepare autologous platelet-rich plasma in the treatment of refractory corneal ulcers. Taiwan J Ophthalmol. 5(3):132-135.

29. Sobecki M, Mrouj K, Colinge J, Gerbe F, Jay P, Krasinska L, Dulic V, Fisher D. 2017. Cell-Cycle Regulation Accounts for Variability in Ki-67 Expression Levels. Cancer Res. 15; 77 (10): 2722-2734.

30. Zhang JM, Feng FE, Wang QM, Zhu XL, Fu HX, Xu LP, Liu KY, Huang XJ, Zhang XH. 2016. Platelet-Derived Growth Factor-BB Protects Mesenchymal Stem Cells (MSCs) Derived From Immune Thrombocytopenia Patients against Apoptosis and Senescence and Maintains MSC-Mediated Immunosuppression. Stem Cells Transl Med. 5 (12):1631-1643.

31. Jang HY, Myoung SM, Choe JM, Kim T, Cheon YP, Kim YM4, Park H. 2017.Effects of Autologous Platelet-Rich Plasma on Regeneration of Damaged Endometrium in Female Rats. Yonsei Med J. 58 (6):1195-1203.

32. Terada S, Ota S, Kobayashi M, Kobayashi T, Mifune Y, Takayama K, Witt M, Vadalà G, Oyster N, Otsuka T, Fu FH, Huard J.2013 .Use of an antifibrotic agent improves the effect of platelet-rich plasma on muscle healing after injury. J Bone Joint Surg Am. 95(11):980-988.

33. Li DQ and Pflugfelder SC. 2005. Matrix metalloproteinases in corneal inflammation. Ocul Surf. 3(4):198-202.

34. Kim YS and Joh TH. 2012. Matrix metalloproteinases, new insights into the understanding of neurodegenerative disorders. Biomol Ther (Seoul). 20(2): 133-143.

35. Silva ML, Ribeiro AP, Silva GA, Sanchez IXB, Renzo R, Uscategui R, Tiago Barbalho Lima, Marcela Aldrovani, José Luiz La Arq. Bras. 2015. Expressions of matrix metalloproteinases-1 and -9 and opioid growth factor in rabbit cornea after lamellar keratectomy and treatment with 1% nalbuphine. Arq Bras Oftalmol. 78(3):141-145

36. Ahmed HH, Rashed LA, Mahfouz S, Elsayed Hussein R, Alkaffas M, Mostafa S, Abusree A. 2017. Can mesenchymal stem cells pretreated with platelet-rich plasma modulate tissue remodeling in a rat with burned skin? Biochem Cell Biol. 95(5): 537-548.

37. Arican M, Şimşek A, Parlak K, Atli K Sönmez G. 2018. Matrix metalloproteinases 2 and 9 activity after intra-articular injection of autologous platelet-rich plasma for the treatment of osteoarthritis in dogs. Acta Vet. Brno. 87: 127-135.

الملخص العربى

دراسة هستولوجية و هستوكيميائية مناعية لتأثير البلازما الغنية بالصفائح الدموية على حرق القرنية الناجم عن القلويات في ذكر الجرذ الأبيض البالغ

هبة السيد محمد شرف الدين، مروة عوض عبد الحميد إبراهيم، نهى رمضان محمد السويدى

قسم الهستولوجيا وبيولوجيا الخلية ـ كلية الطب ـ جامعة طنطا

مقدمة: الإصابات الكيميائية للعين هي حالة طارئة تحتاج إلى تقييم وعلاج فورى ومكثف. و قد أصبحت البلازما الغنية بالصفائح الدموية علاجًا شائعًا في مجال جراحة العيون.

الهدف من العمل: تقييم ومقارنة تأثير حقن جرعة واحدة من البلازما الغنية بالصفائح الدموية يتم حقنها إما بعد ساعتين أو 48 ساعة على حرق القرنية الناجم عن القلويات.

مواد و طرق البحث: تم تقسيم ثلاثين من ذكور الجرذان البيضاء البالغة بشكل متساوٍ إلى خمس مجموعات: الضابطة، المعالجة بالبلازما الغنية بالصفائح الدموية, مجموعة حرق القرنية الناجم عن القلويات, مجموعة حرق القرنية الناجم عن القلويات + البلازما الغنية بالصفائح الدموية بعد ساعتين و مجموعة حرق القرنية الناجم عن القلويات + البلازما الغنية بالصفائح الدموية بعد 48 ساعة. وتمت معالجة عينات القرنية للتقنيات الهستولوجية والهستوكيميائية المناعية المختلفة.

النتائج: أظهر الحرق القلوى للقرنية بؤر من إنقطاع التواصل والتعرية للنسيج الطلائى للقرنية بالتناوب مع بؤر من عدم الترتيب و التطبق. بدا غشاء بومان غير منتظم مع بؤر من إضطراب التنسيق. بينما بدا غشاء ديسمت رقيق السماكة و مضطرب التنسيق. وقد لوحظ تخلل من الخلايا وحيدة النواة و اجتياح من الأوعية الدموية الصغيرة. عند العلاج بالبلازما الغنية بالصفائح الدموية بعد ساعتين من الحرق القلوى ، لوحظ وجود هيكل نسيجى للقرنية قريب من الطبيعى. ولكن بعد العلاج بالبلازما الغنية بالصفائح الدموية بعد مرور 48 ساعة من الحرق القلوى ، تم الكشف عن بنية نسيجية مضطربة للقرنية مع نسيج طلائى مفرغ وبعض التغيرات في الأنوية. تم الكشف عن إختلاف ذي دلالة إحصائية عالية في الصبغة الهستوكيميائية المناعية للكشف عنMMP-1، Ki67 ، P53 و MMP-9 في مجموعة الحرق القلوى مقارنة مع المجموعة الضابطة، في حين لوحظ إختلاف غير ذى دلالة إحصائية في المجموعة الرابعة مقارنة بالمجموعة الضابطة ، بينما تم الكشف عن إختلاف ذي دلالة إحصائية بين المجموعة الخامسة و المجموعة الضابطة.

الاستنتاج: كان العلاج بحقن جرعة واحدة من البلازما الغنية بالصفائح الدموية له تأثير مخفف لحرق القرنية الناجم عن القلويات، ولكن حقن البلازما الغنية بالصفائح الدموية بعد ساعتين من الحرق كان أكثر كفاءة في إستعادة السطح الصحى للقرنية بشكل أفضل من حقنها بعد 48 ساعة.